Electronic Supplementary Material (ESI) for Dalton Transactions.

An Exhibition of the Brønsted Acid-Base Character by a Schiff Base in Palladium(II) Complex Formation: Lithium Complex, Fluxional Property and Catalysis of Suzuki Reactions in Water

*Rajnish Kumar and Ganesan Mani**

Department of Chemistry, Indian Institute of Technology – Kharagpur, Kharagpur, West Bengal,

India 721 302, Fax: +91 3222 282252, E-mail: gmani@chem.iitkgp.ernet.in.

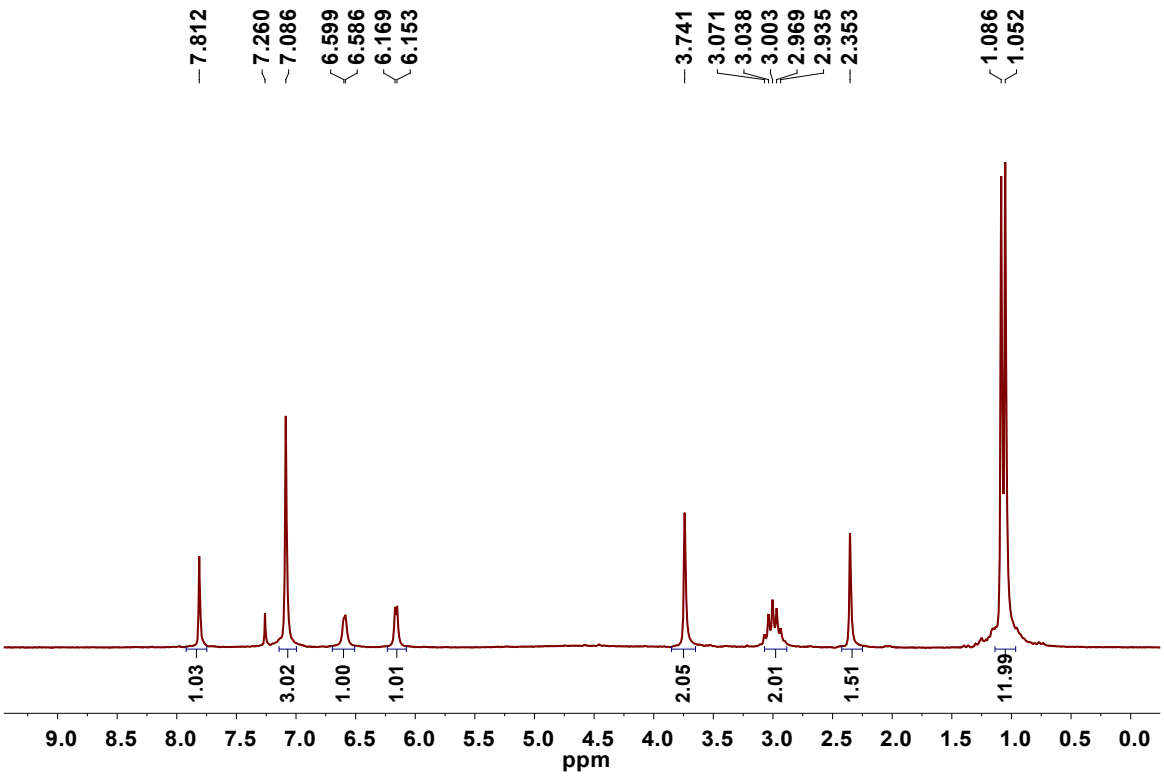

Figure S1. ^{1}H-NMR spectrum of bis(iminopyrrolylmethyl)amine **H_2L** in $CDCl_3$.

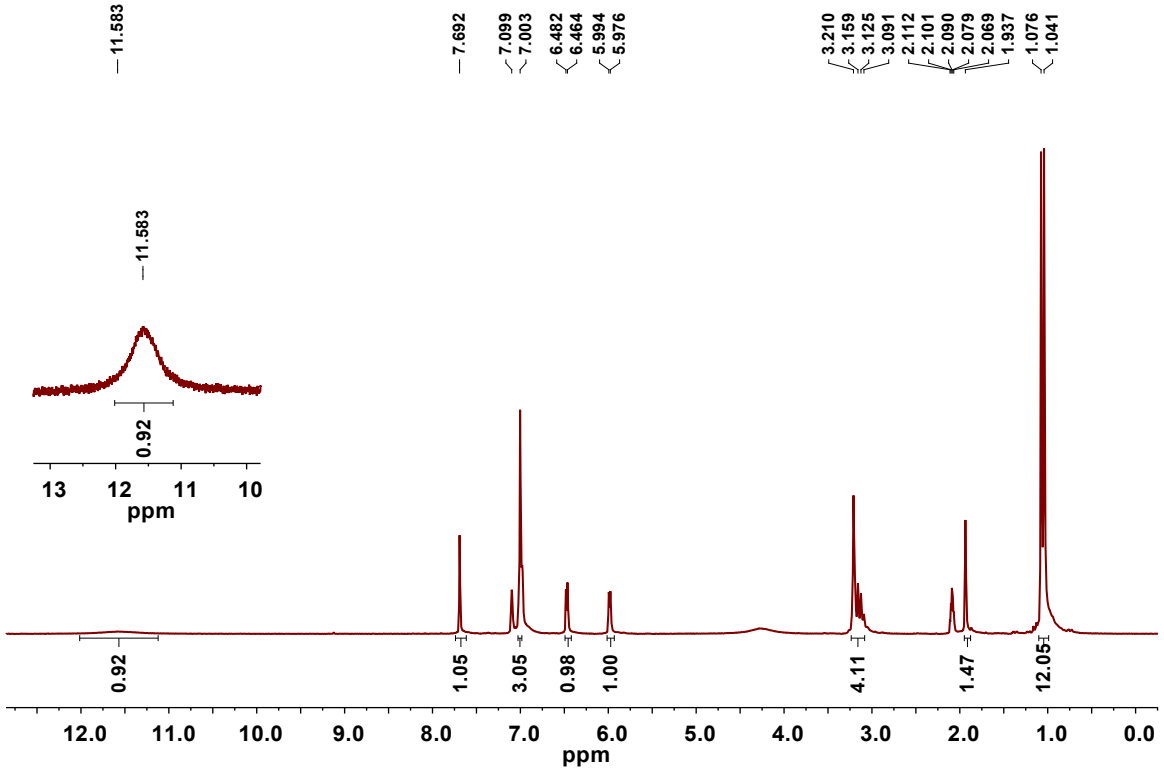

Figure S2. ^{1}H-NMR spectrum of bis(iminopyrrolylmethyl)amine **H_2L** in toluene-d_8. The broad peak round δ 4.25 ppm is probably due to water.

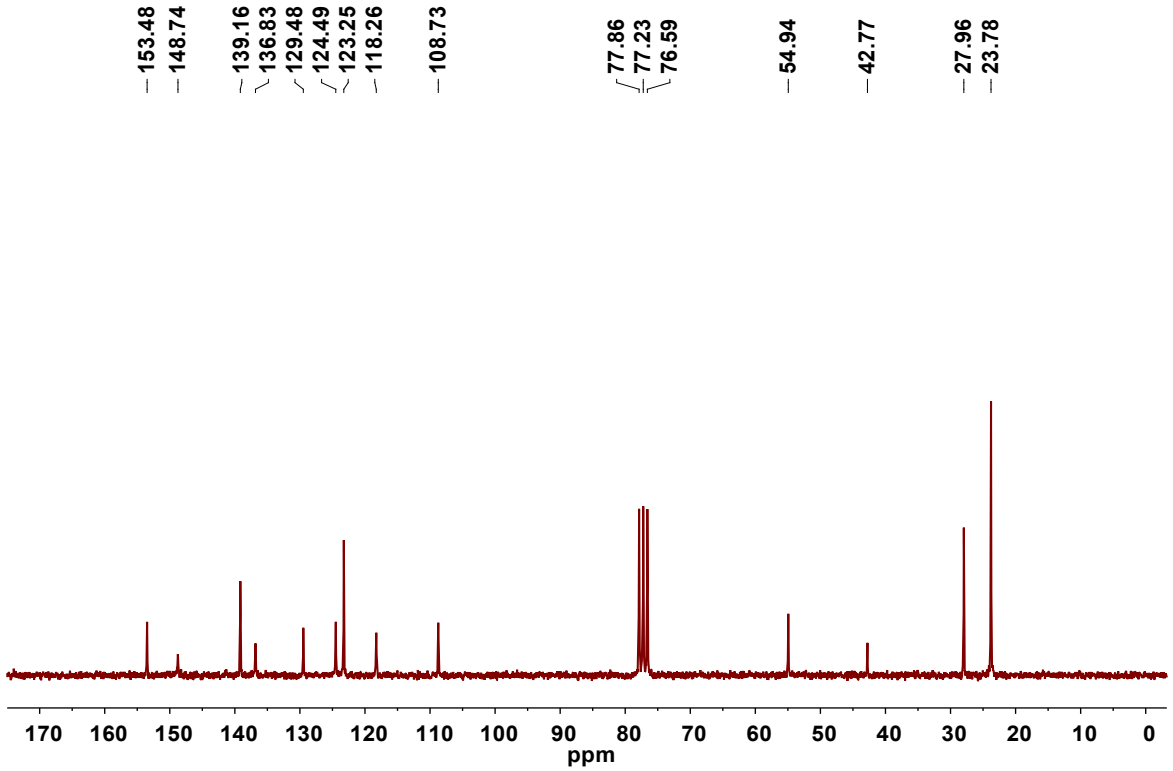

Figure S3. $^{13}C\{^{1}H\}$-NMR spectrum of bis(iminopyrrolylmethyl)amine **H_2L** in $CDCl_3$.

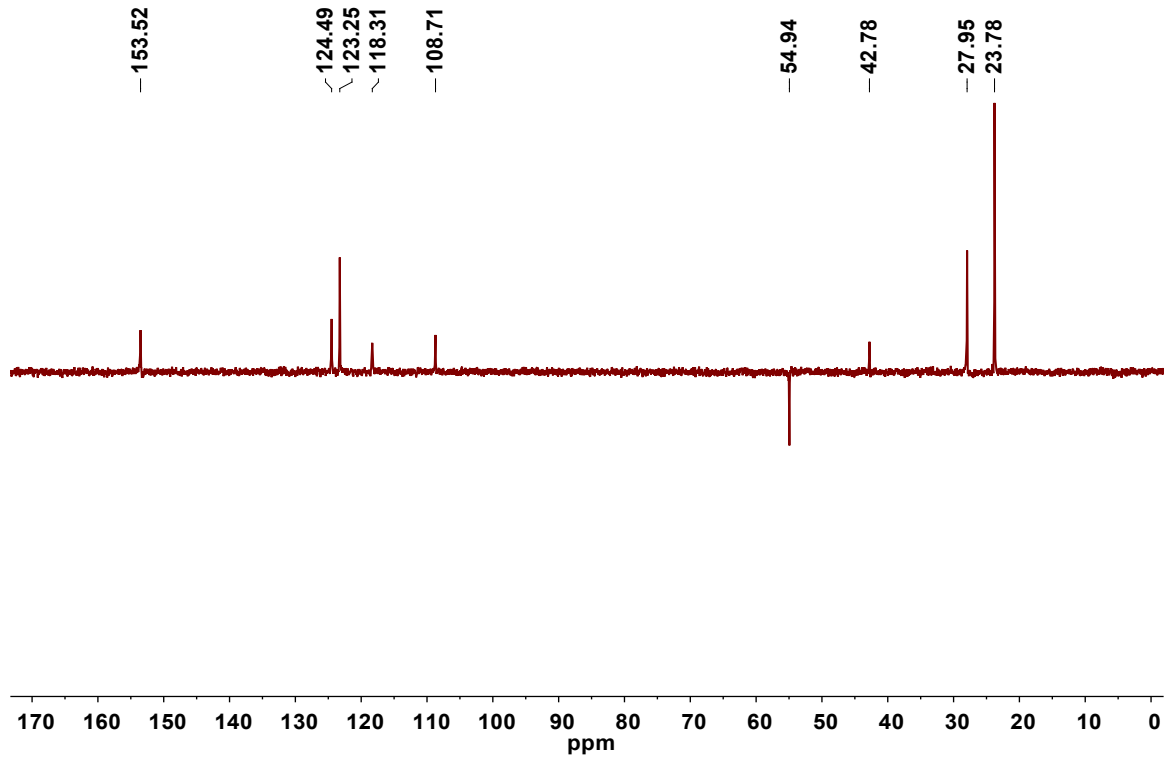

Figure S4. DEPT$\{^{1}H\}$-135 NMR spectrum of bis(iminopyrrolylmethyl)amine **H_2L** in $CDCl_3$.

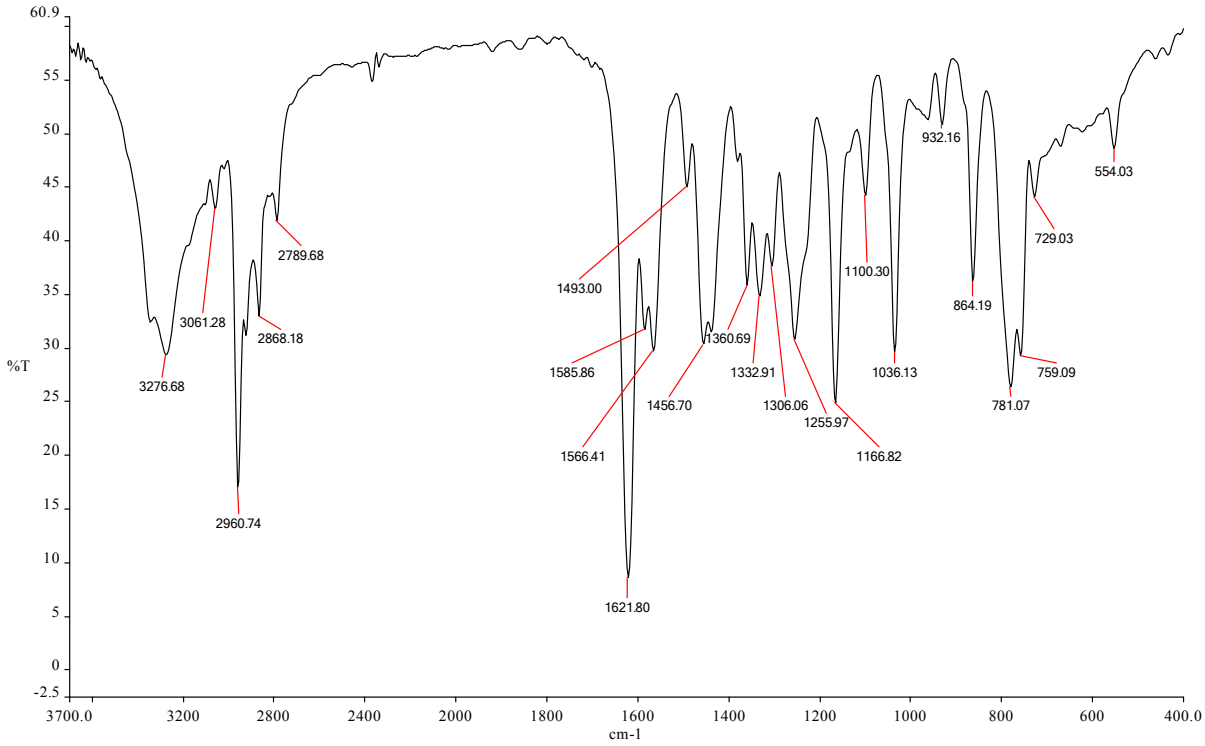

Figure S5: FTIR spectrum of bis(iminopyrrolylmethyl)amine **H_2L** recorded as a KBr disc.

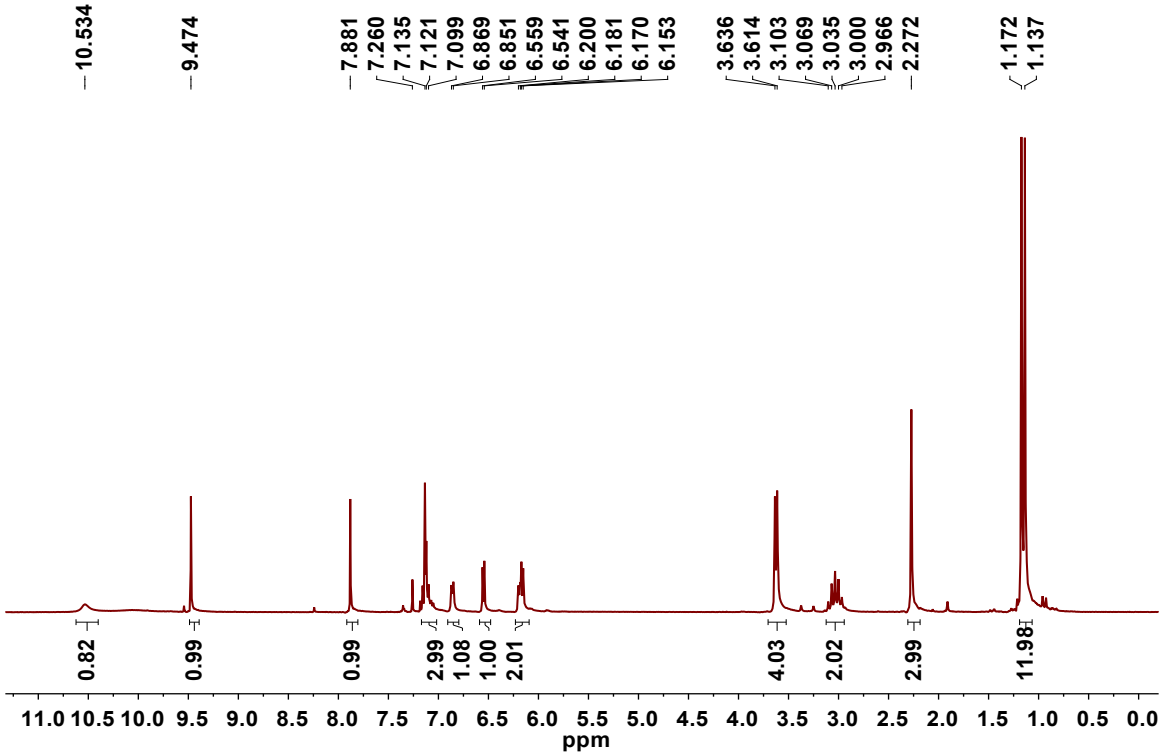

Figure S6. ^{1}H-NMR spectrum of the monoimino compound **H_2L'**in $CDCl_3$.

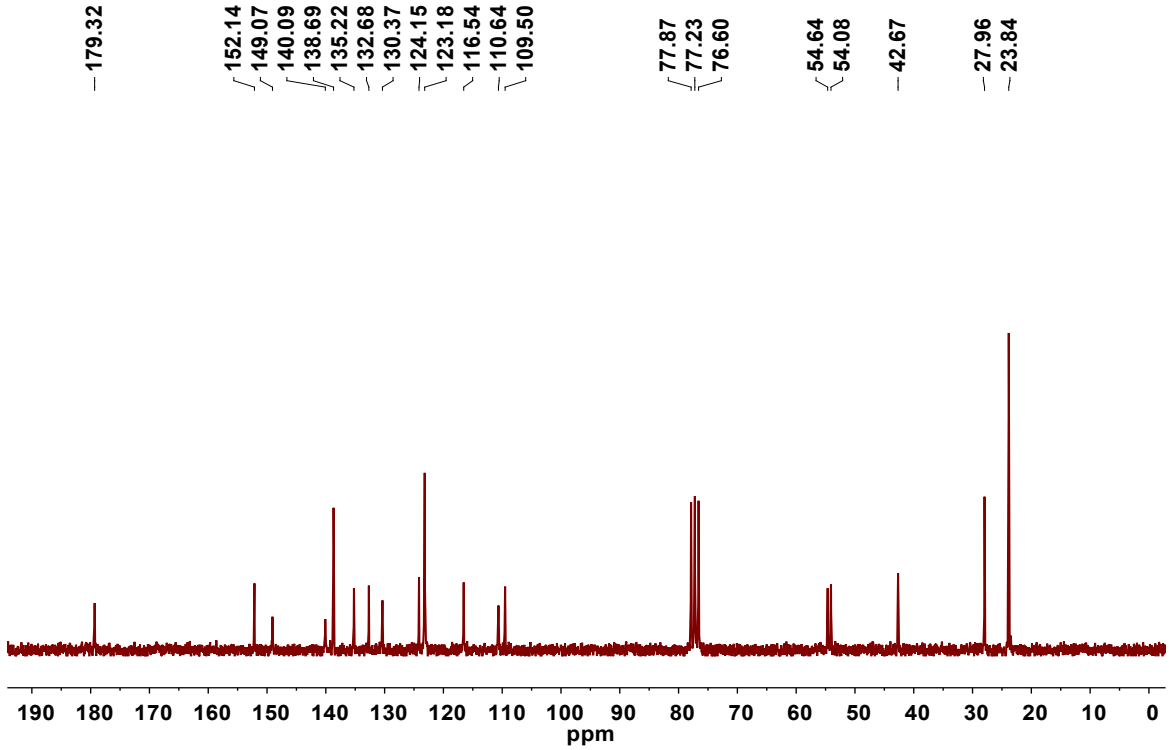

Figure S7. $^{13}C\{^{1}H\}$-NMR spectrum of the monoimino compound **H_2L'** in $CDCl_3$.

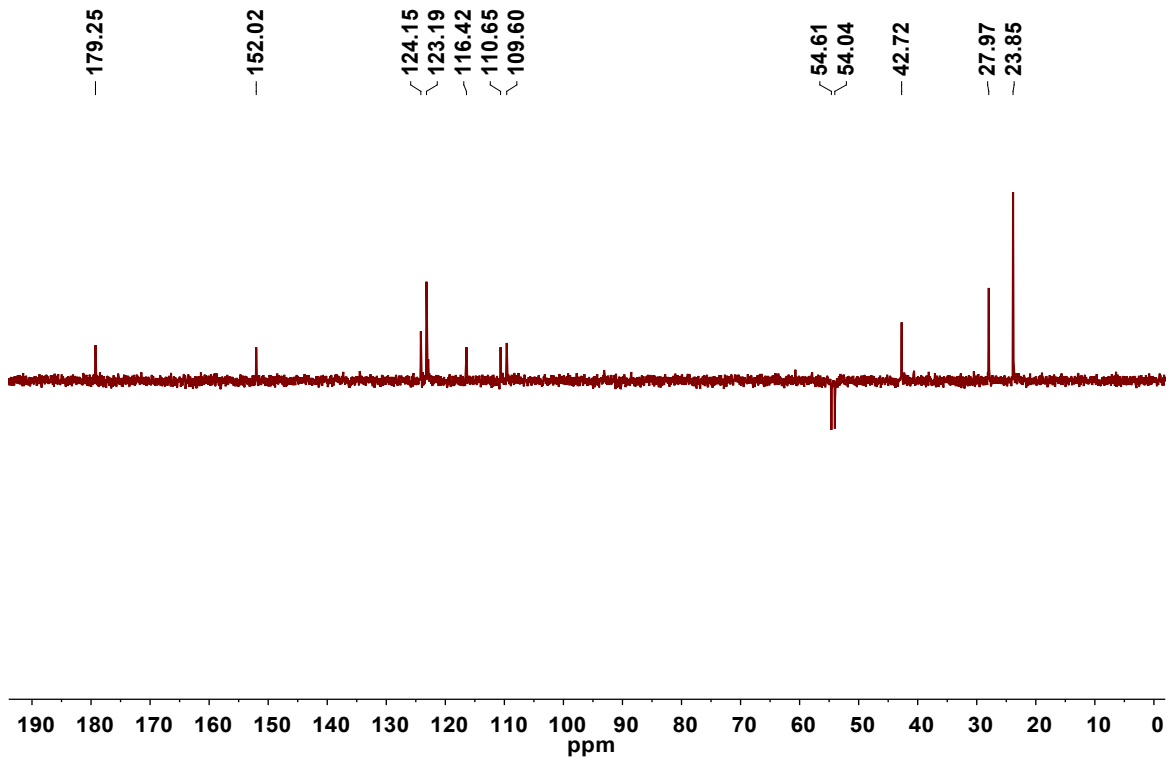

Figure S8. DEPT$\{^{1}H\}$-135 NMR spectrum of the monoimino compound **H_2L'** in $CDCl_3$.

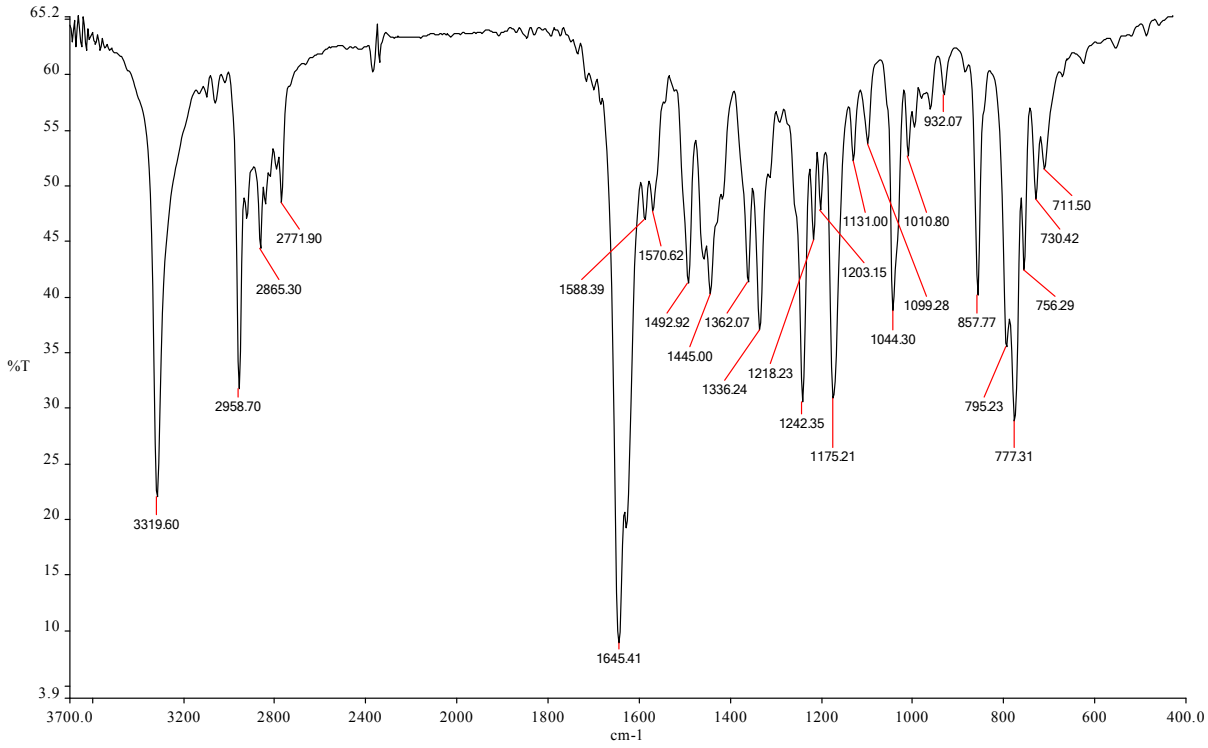

Figure S9: FTIR spectrum of the monoimino compound **H_2L'** recorded as a KBr disc.

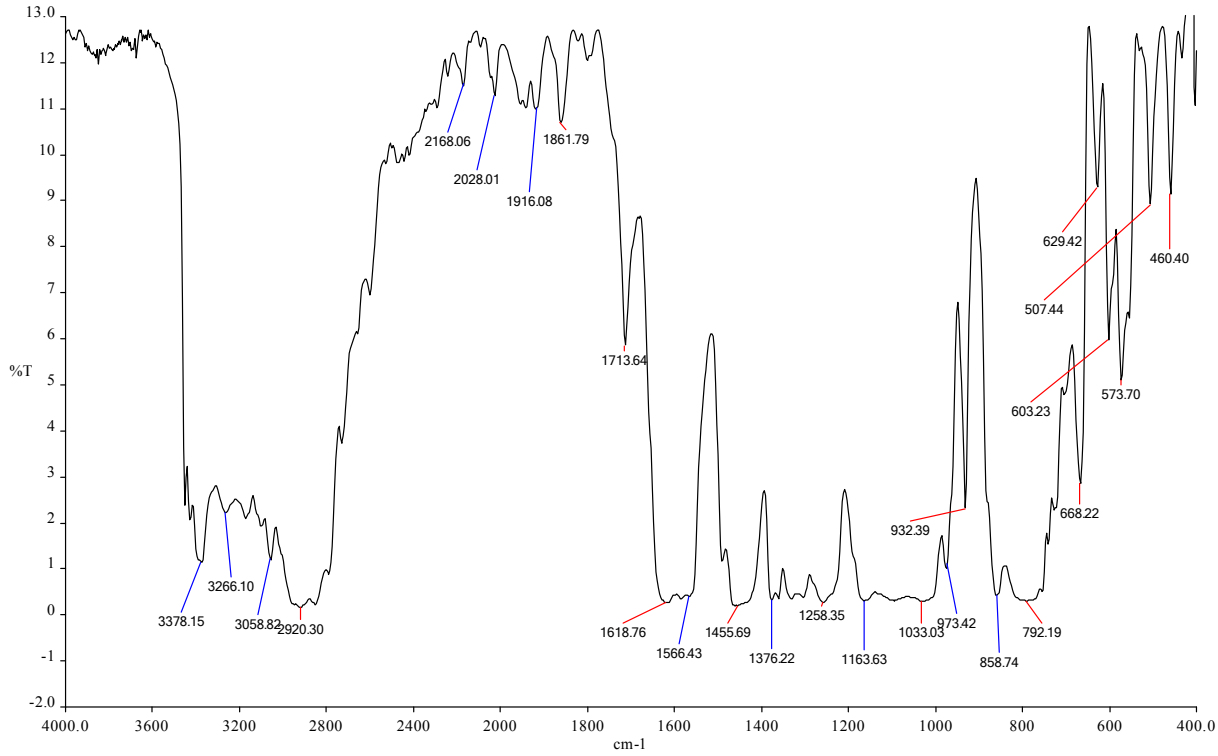

Figure S10: FTIR spectrum of the dimeric lithium complex **2** recorded as a Nujol mull.

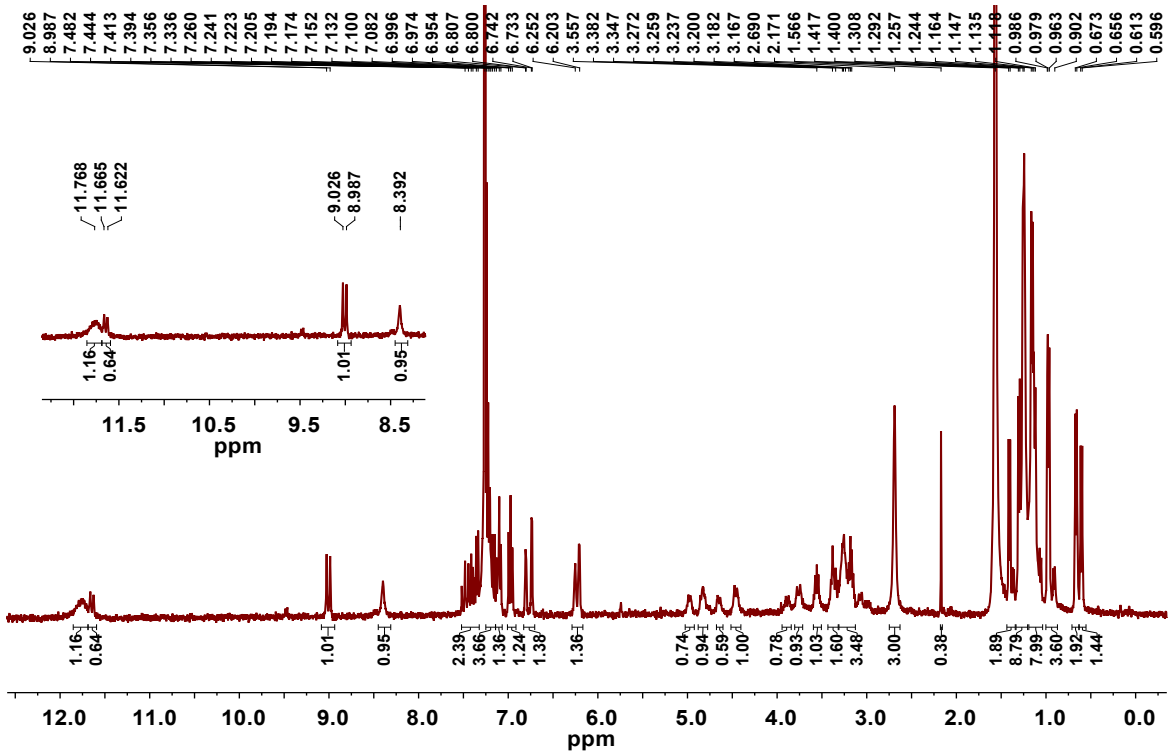

Figure S11. ^{1}H-NMR spectrum of the cationic Pd(II) complex **3** in $CDCl_3$.

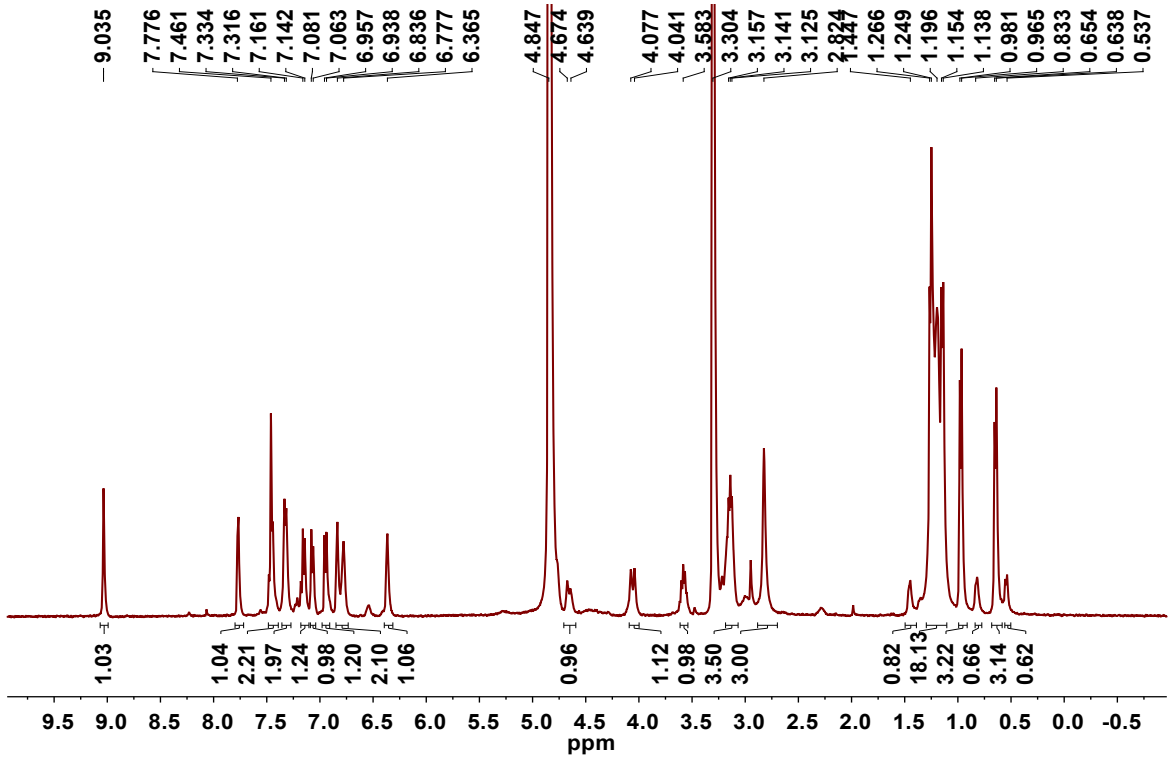

Figure S12. ^{1}H-NMR spectrum of the cationic Pd(II) complex **3** in methanol-d_4.

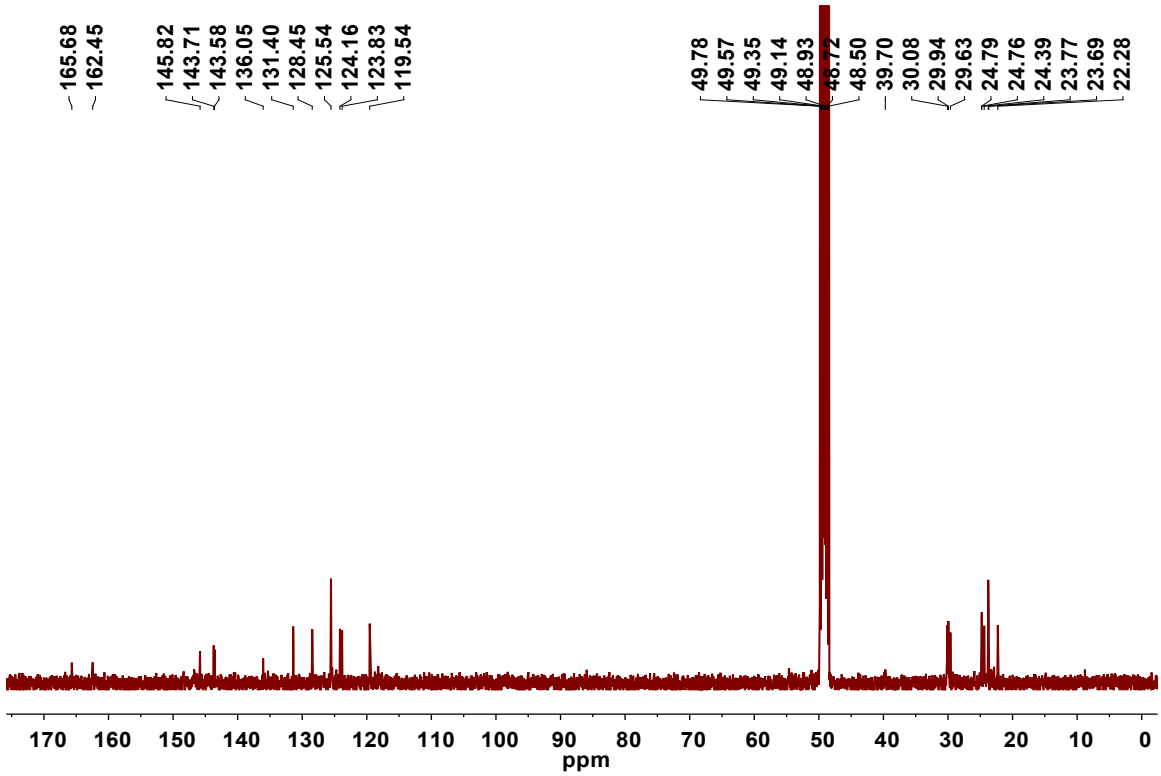

Figure S13. $^{13}C\{^{1}H\}$-NMR spectrum of the cationic Pd(II) complex **3** in methanol-d_4.

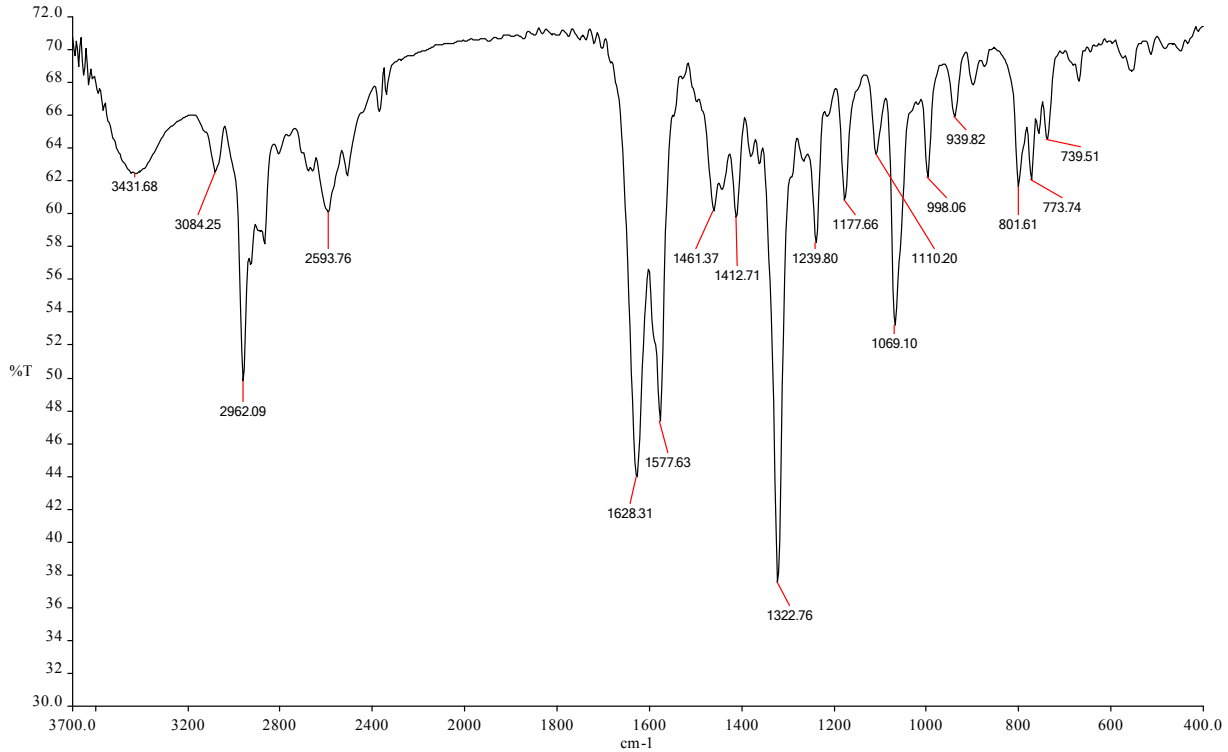

Figure S14: FTIR spectrum of the cationic Pd(II) complex **3** recorded as a KBr disc.

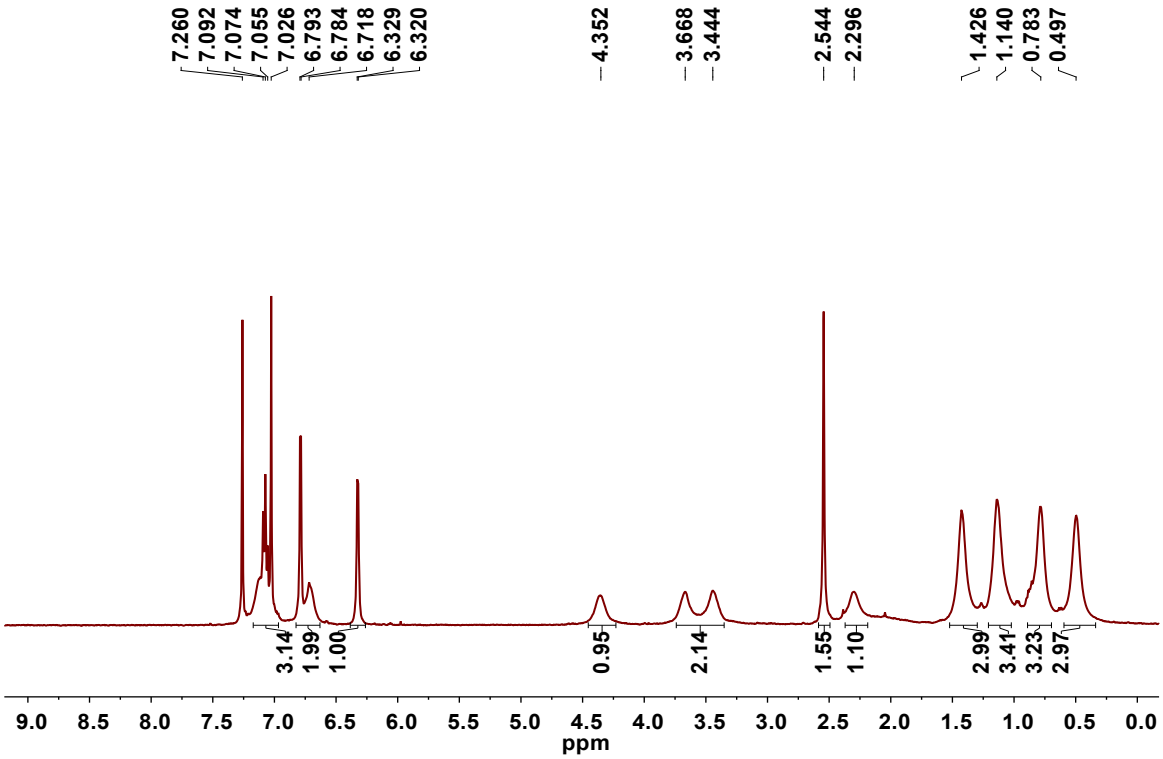

Figure S15. ^{1}H-NMR spectrum of the neutral Pd(II) complex **4** in $CDCl_3$ at 23 °C.

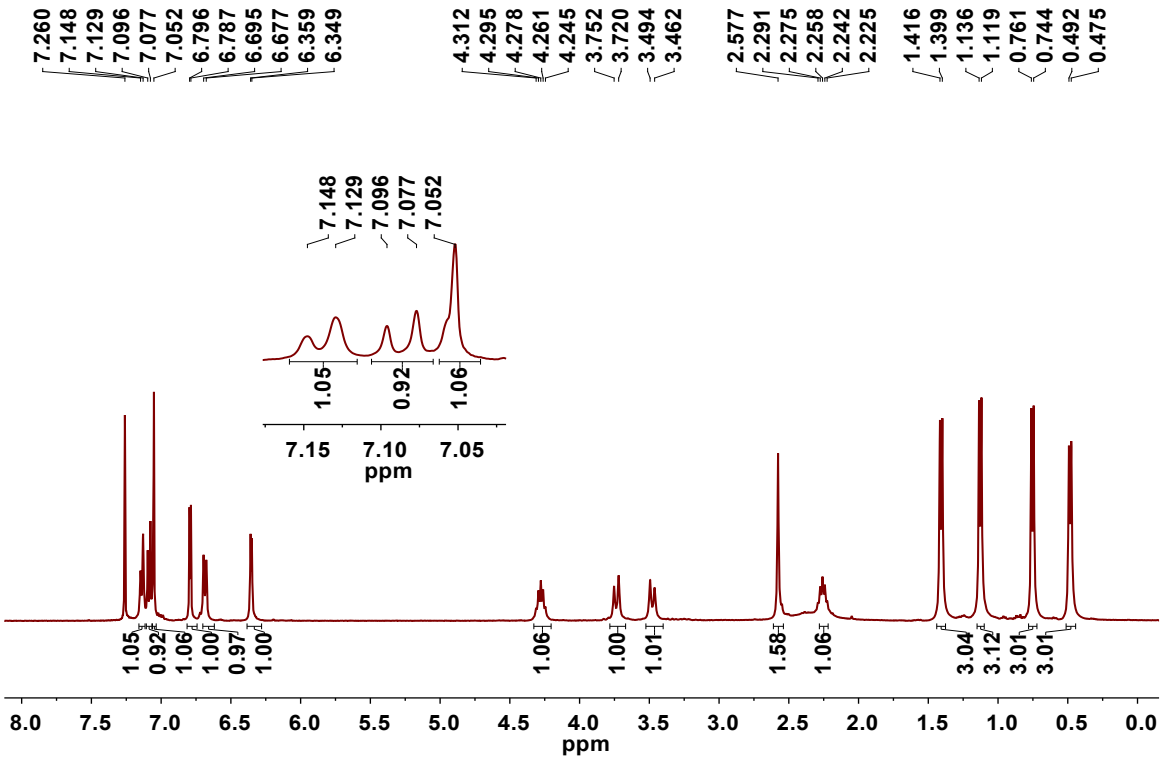

Figure S16. ^{1}H-NMR spectrum of the neutral Pd(II) complex **4** in $CDCl_3$ at 0 °C.

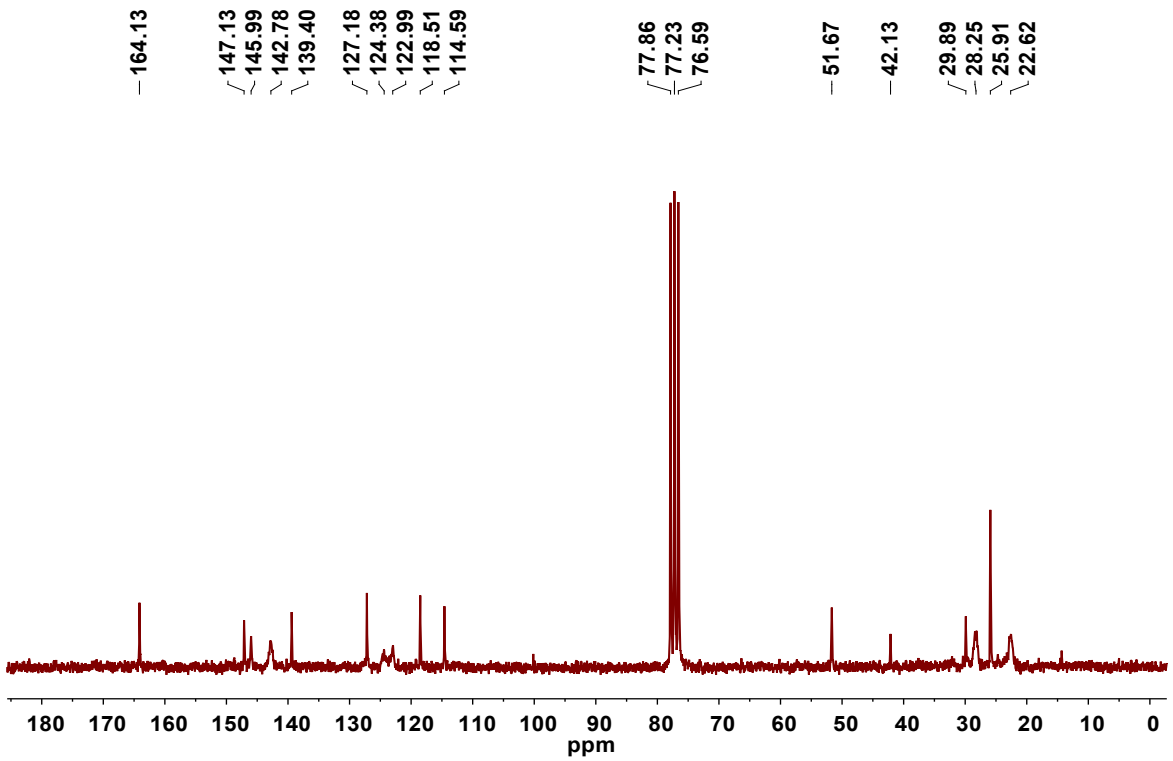

Figure S17. $^{13}C\{^{1}H\}$-NMR spectrum of the neutral Pd(II) complex **4** in $CDCl_3$.

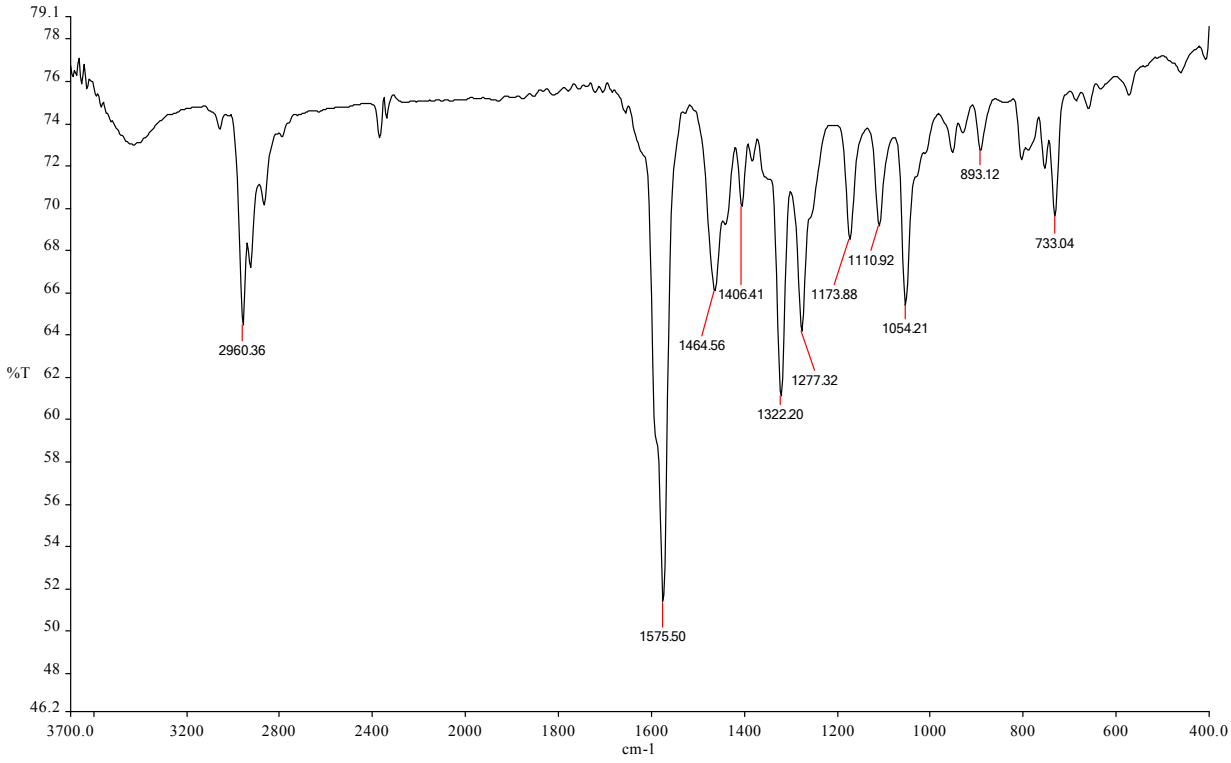

Figure S18: FTIR spectrum of the neutral Pd(II) complex **4** recorded as a KBr disc.

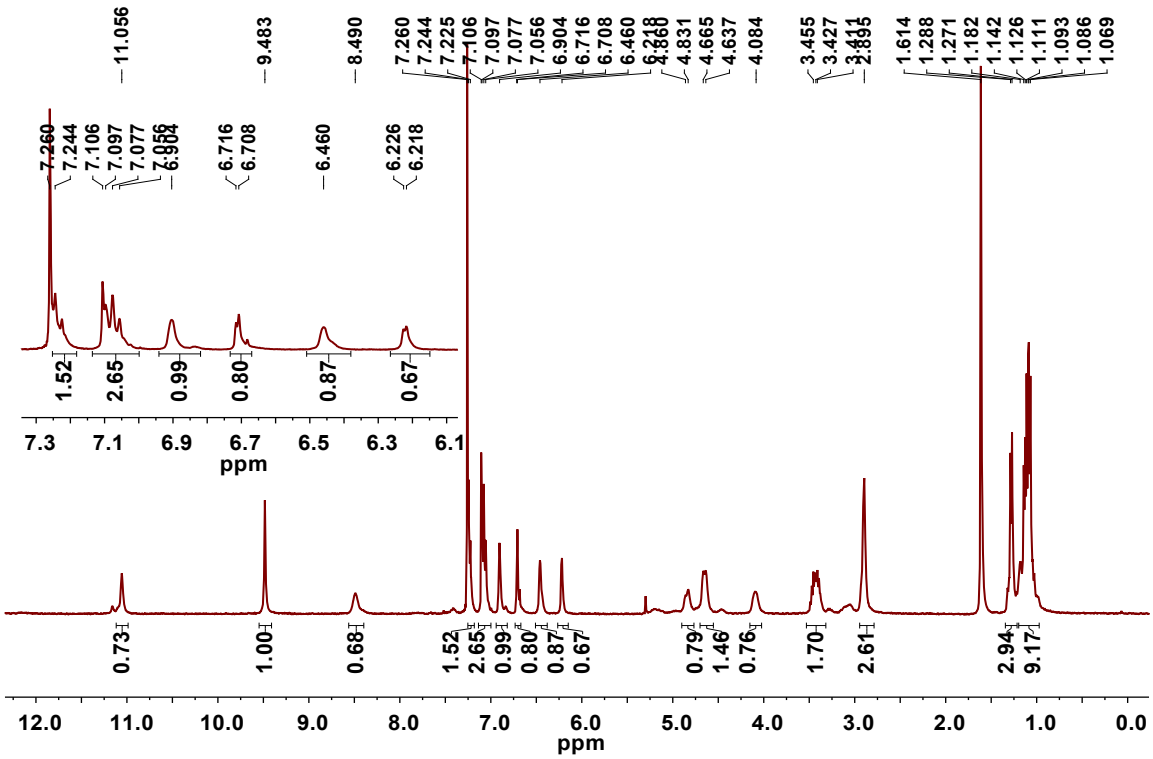

Figure S19. ^{1}H-NMR spectrum of the zwitterionic Pd(II) complex **5** in $CDCl_3$.

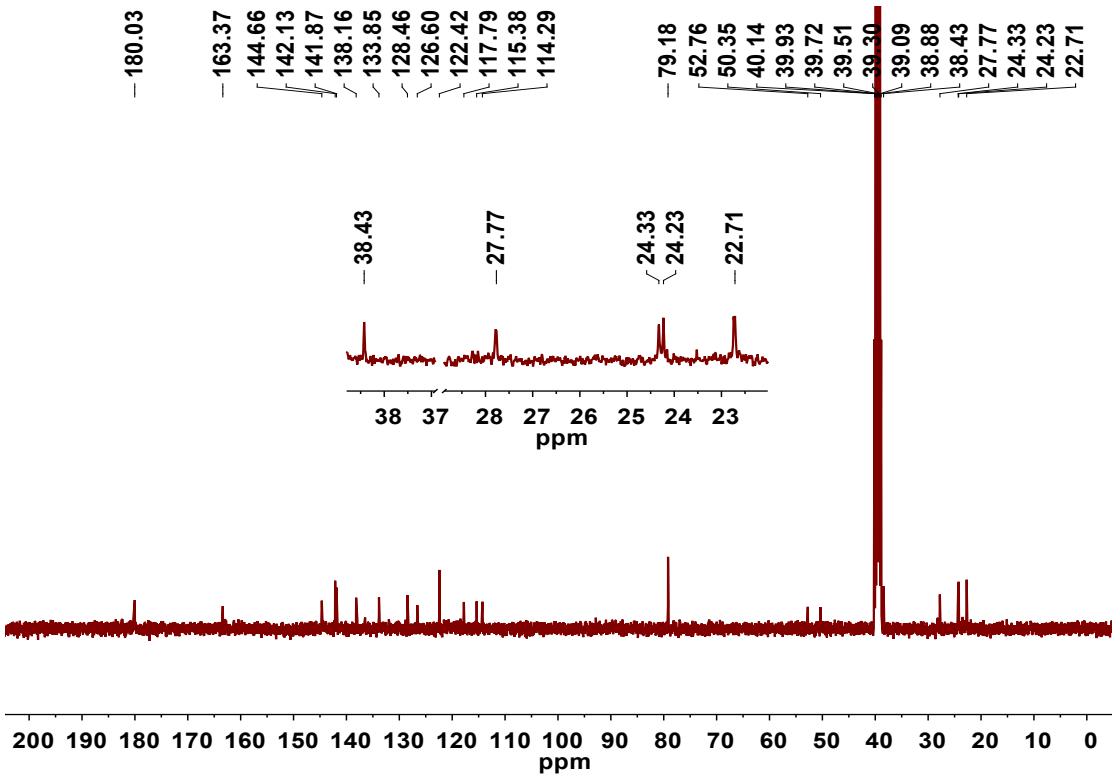

Figure S20. $^{13}C\{^{1}H\}$-NMR spectrum of the zwitterionic Pd(II) complex **5** in dmso-d_6.

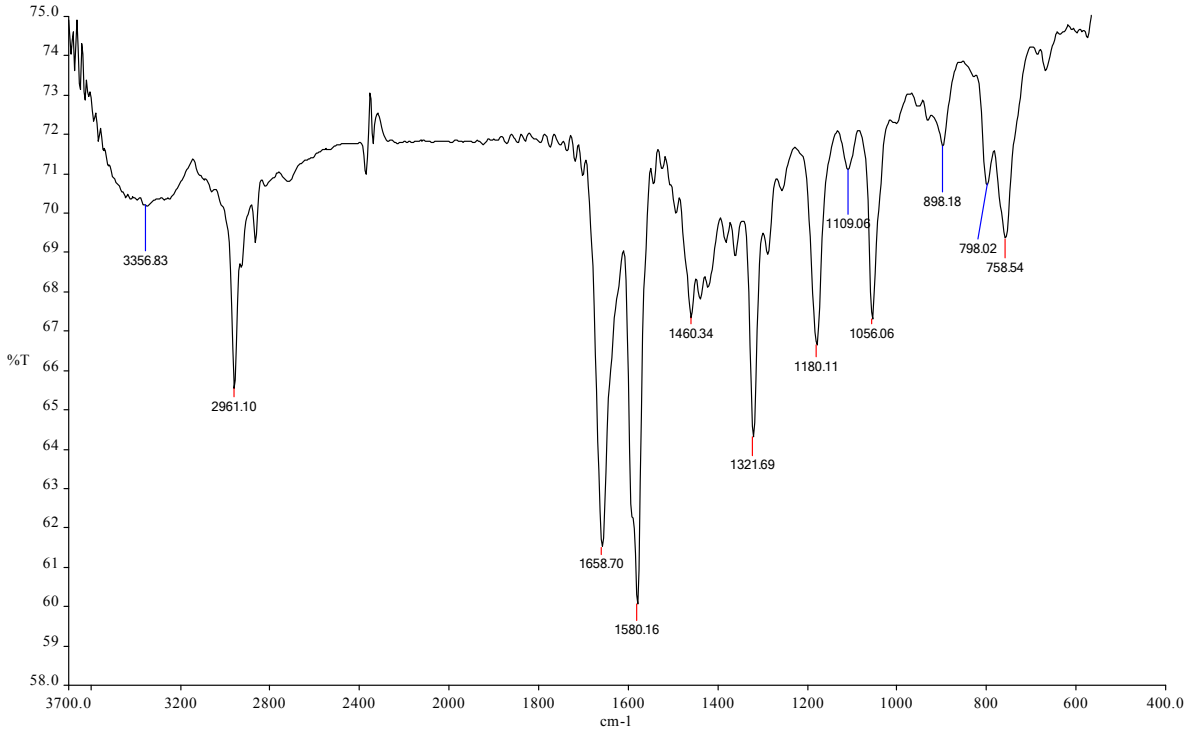

Figure S21: FTIR spectrum of the zwitterionic Pd(II) complex **5** recorded as a KBr disc.

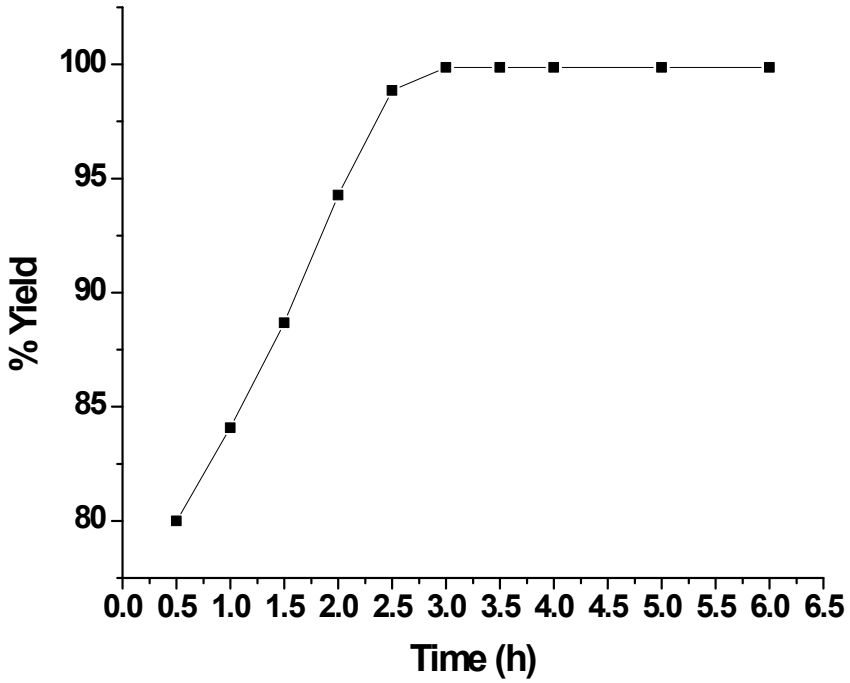

Figure S22. Plot of time vs yield for the Suzuki-Miyaura coupling between 4-bromoacetophenone and phenylboronic acid. A round bottom flask containing 4-bromoacetophenone (1 mmol), phenylboronic acid (1.5 mmol), K_2CO_3 (2 mmol), catalyst **3** (0.01 mol%), and H_2O (1.5 mL) was placed in a oil bath which is already preheated to 100 °C. The reaction was stopped for every 30 minutes, and the product was separated and the yield was calculated as mentioned in the general procedure of the Suzuki reaction.

X-ray structures

Table 1 Crystallographic data for **H_2L**·H_2O and **H_2L'.**

	H_2L·H_2O	**H_2L'**
Empirical formula	$C_{37}H_{51}N_5O$	$C_{25}H_{32}N_4O$
Formula weight	581.83	404.55
Wavelength (Å)	0.71073	0.71073
Temperature (K)	293(2)	293(2)
Crystal system	Triclinic	Triclinic
Space group	$P\bar{1}$	$P\bar{1}$
a/Å	10.429(4)	9.0287(16)
b/Å	13.208(5)	9.7736(18)
c/Å	14.228(5)	14.728(3)
α/degree	71.233(11)	95.194(6)
β/degree	84.201(12)	91.309(6)
γ/degree	76.698(11)	113.379(5)
Volume (Å^3)	1805.1(11)	1185.6(4)
Z	2	2
D_{calcd} , g cm^{-3}	1.070	1.133
μ/mm^{-1}	0.065	0.071
F(000)	632	436
θ range (degree)	1.51 to 24.87	2.28 to 25.00
Limiting indices	–11<=h<=12, –14<=k<=15, –16<=l<=16	–9<=h<=10, –11<=k<=11, –17<=l<=17
Total/ unique no. of reflns.	21315 / 6222	14316 / 4163
R_{int}	0.0955	0.0529
Data / restr./ params.	6222 / 2 / 401	4163 / 0 / 278
GOF (F^2)	1.004	1.002
R1, *wR2*	0.0724, 0.1610	0.0606, 0.1568
R indices (all data) *R1*, *wR2*	0.1863, 0.2117	0.1195, 0.1938
Largest different peak and hole (e Å^{-3})	0.221 and –0.161	0.526 and –0.273

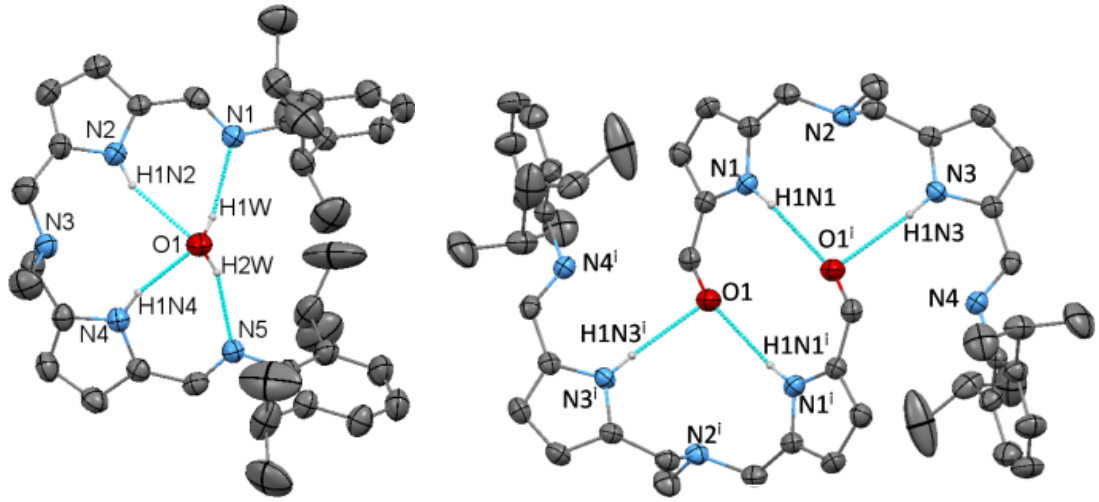

Figure S23. The X-ray structure of $\mathbf{H_2L}\cdot H_2O$ (a) and the hydrolyzed monoimino compound $\mathbf{H_2L'}$ which forms the intermolecular hydrogen bonds in the crystal lattice (b). Dotted lines indicate hydrogen bonds. Most hydrogen atoms are omitted for clarity. Selected bond lengths [Å] and angles [º] for $\mathbf{H_2L}$: N2···O1 2.998(4), H1N2···O1 2.16(4), N2–H1N2···O1 159(3), N4···O1 2.870(4), H1N4···O1 2.00(4), N4–H1N4···O1 166(3), O1···N1 2.842(4), H1W···N1 2.05(2), O1–H1W···N1 163(4), O1···N5 2.859(4), H2W···N5 2.06(2), O1–H2W···N5 160(4). For $\mathbf{H_2L'}$: N1···O1^{i} 2.988(3), H1N1···O1^{i} 2.16(3), N1–H1N1···O1^{i} 162(3), N3···O1^{i} 3.161(3), H1N3···O1^{i} 2.30(3), N3–H1N3···O1^{i} 176(3). The symmetry operation used to generate equivalent atoms: –x+2, –y, –z+1.